Broadband Beam Steering

J. E. Stockley[a], S. A. Serati[b], G. D. Sharp[b], P. Wang[b], K. F. Walsh[c] and K. M. Johnson[a]

[a] Optoelectronic Computing Systems Center, University of Colorado,
Campus Box 525 Boulder CO 80309-0525

[b] Boulder Nonlinear Systems, Inc. 1898 S. Flatiron Court Boulder CO 80301

[c] Rochester Photonics Corporation, 330 Clay Road Rochester NY 146123

ABSTRACT

A solid-state broadband beam deflector is described. This non-mechanical system steers spatially coherent broad band light to a common location in the far field. The components include a liquid crystal grating and achromatic Fourier transformer. The liquid crystal grating employs a polarization modulation scheme which produces a wavelength independent phase shift. The achromatic Fourier transformer eliminates grating dispersion.

The modulation theory for the liquid crystal grating is introduced. Observations of the far field patterns for white light illumination of a binary liquid crystal grating and the design for the achromatic Fourier transformer are presented. Future research, including mid-infrared implementation is discussed.

Keywords: broadband beamsteering liquid crystal gratings

1. INTRODUCTION

When used as a receiver, a beam deflector can steer the field of view of a passive sensor, resulting in greater resolution without losing angular coverage. Analogous to tilting a mirror, this scanning is accomplished by producing a wedge shaped phase front across the beam. Imaging using a broadband sensor requires the beam scanner to operate over a broad spectral range of wavelengths.

Beam steering can be achieved with liquid crystal writable gratings[1]. However, the diffractive grating structure and the chromatic nature of the phase modulating mechanism have restricted broadband implementation to microradian steering angles[2]. One solution is to use an achromatic Fourier transformer and an array of broadband phase shifters[3].

An optical phased array is conveniently implemented using a liquid crystal writable grating. Ideally the phase profile produced by the grating emulates a linear ramp using a periodic saw-tooth function having a 2π modulation depth. A grating is a dispersive element. That is, the diffraction angles are a function of wavelength, λ. In the far field the first order diffraction angle, θ_1, is given by

$$\sin\theta_1 = \frac{\lambda}{L} \tag{1}$$

where L is the grating period. We refer to the first diffracted order as the scanner's view angle. Other orders, or sidelobes, are not desirable in most applications. Equation 1 shows that the view angle is wavelength dependent. This presents a problem for a scanner which is supposed to direct broadband energy to a single point.

Grating dispersion can be resolved by using an achromatic Fourier transformer. Spatially coherent achromatic Fourier transformers have been investigated in the past because of their unique treatment of broadband light. This type of lens system scales broadband light from a common location in one focal plane to a common spatial resolution in another. It should not be confused with an achromatic lens since they perform the opposite function (i.e. one produces lateral color while the other eliminates it). A three lens system has previously been developed which produces an achromatic transformation that is (paraxially) well corrected over the entire visible spectrum[4,5].

A second obstacle to broadband scanning using a writable grating is that the relative amplitude between the first order and sidelobes is also a function of wavelength if the phase modulating elements of the grating are dispersive. If the phase profile is an ideal linear ramp with resets modulo 2π, then at the design wavelength of the modulating elements all of the energy is diverted into the first diffracted order. However, at other wavelengths, the dispersive nature of the phase shifting elements results in increased sidelobe amplitude. Consider a single period of the saw-tooth phase grating. The transmittance as a function of position, x, can be described by

$$t = e^{-i\left(\frac{\pi+\delta}{L/2}\right)x} \tag{2}$$

where δ is the chromatic error resulting in a deviation in the phase modulation depth from 2π. Calculating the Fourier series of Equation 2 gives the intensity transmission of the phase grating in the first diffracted order as

$$T_1 = \left(\frac{\sin\delta}{\delta}\right)^2 \quad . \tag{3}$$

Equation 3 demonstrates that the amplitude of the first diffracted order decreases for wavelengths other than the design wavelength of the phase shifting elements. This increases the sidelobe amplitudes and produces a non-diffracted component. Energy lost to undesired orders is not only an efficiency problem, it also causes system-level errors such as image blurring and interference from sources outside the desired angle of acceptance.

The wavelength dependence of the phase shifting elements can be minimized by using a chiral smectic liquid crystal (CSLC) writable grating. These devices operate on the principle of topological phase shift. That is, manipulation of the polarization produces a change in optical phase. This polarization modulation is accomplished by re-orientation of the optic axis in a plane transverse to the direction of propagation in a manner similar to mechanical rotation of a waveplate. With a CSLC waveplate, the molecular tilt in the transverse plane changes as a function of applied electric field. This rotates the optic axis of the CSLC modulator. The position of the optic axis is the same for all wavelengths and ideally so is the induced phase shift.

Broadband beamsteering can be achieved using an array of achromatic phase shifters (such as a chiral smectic liquid crystal writable grating) and an achromatic Fourier transformer. Below it is demonstrated that chiral smectic liquid crystal modulators can produce a broadband phase shift, and that an achromatic Fourier transformer compensates for grating dispersion. A schematic of a broadband scanner configuration which consists of an achromatic Fourier transformer and a chiral smectic liquid crystal writable grating is shown in Figure 1.

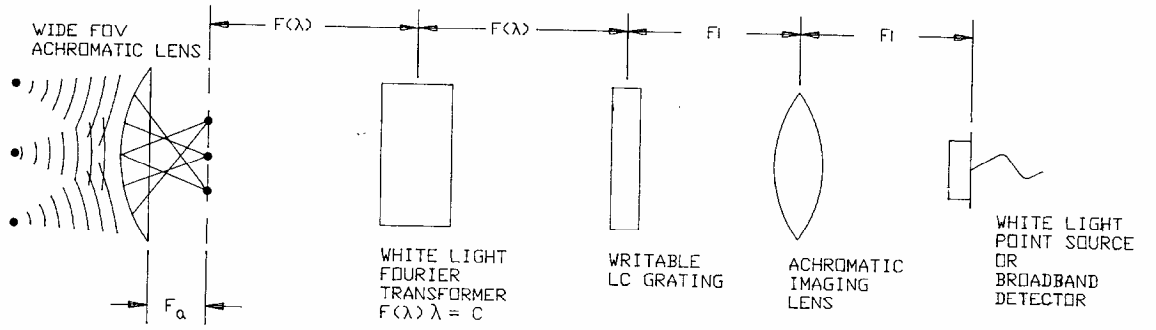

Figure 1. Broadband beam scanning configuration.

2. PHASE SHIFTERS

2.1 Nematic phase shifters

First consider the homogeneous aligned nematic liquid crystal modulators used in conventional liquid crystal writable gratings. For homogeneous aligned nematic liquid crystals a phase shift is achieved by modulating the extraordinary index of refraction of the material. The mechanism is a rotation of anisotropic molecules in a plane containing the device normal. An extraordinary input sees a voltage variable refractive index which decreases from a maximum $n_e(0)$ in the zero-field state and approaches the ordinary index n_o in the fully energized state. Since the input is an Eigenpolarization, the result is a pure phase shift with no change in the state of polarization. For an out-of-plane tilt angle α, and a maximum phase shift of 2π the complex transmittance of the nematic modulator is given by

$$t_{xx} = e^{-i2(\pi+\delta)\left[\frac{n_e(\alpha)}{n_e(0)-n_o}\right]} \quad . \tag{4}$$

Most of the dispersion is associated with the passive phase shift of the device, or the common phase (not unlike the glass substrate). Arbitrarily defining the phase shift in the unenergized state as zero, the modulation depth is given by

$$\Delta\Phi = -2\left(\pi+\delta\right) \quad . \tag{5}$$

To facilitate a direct comparison with the rotative phase shifter schemes to follow, we can re-write the complex transmission of the nematic modulator of Equation 4 as

$$t_{xx} = e^{-i4\alpha\left(1+\frac{\delta}{\pi}\right)} \quad . \tag{6}$$

2.2 Rotative phase shifter element design

The active portion of the phase shifter elements consists of a CSLC zero-order half-wave retarder designed for a central wavelength in the desired spectral band. Chiral smectic liquid crystals act as rotative waveplates of relatively constant retardation. Application of an electric field in the direction of the device normal results in rotation of the optic axis in the transverse plane.

For phase shifters based on the topological phase the state of polarization of the light traverses a closed circuit on the Poincare' sphere, with phase shift determined only by the orientation of a half-wave retarder. This phase shift is wavelength independent, provided that the individual components are themselves achromatic.

The design effort has focused on identifying and theoretically evaluating the best-form reflection mode phase-shifter scheme. The design assumes a pure rotative (or in-plane rotation) CSLC device with a full molecular rotation angle of 90^o. This is coupled with whatever passive polarization optics best produce a phase only modulation, with phase shift independent of wavelength. For each design considered here, Figure 2 shows both the reflection mode version, and the unfolded version. The latter is shown because it is often simpler to appreciate the modulation scheme by observing the unfolded version.

The highest priority is to identify a design that provides the desired full-wave of phase modulation, with as little phase shift dispersion as possible. A lesser priority, but still of importance, is to identify the design that minimizes amplitude modulation. Amplitude modulation is manifested by a conversion of light to the orthogonal polarization. While this component can contaminate the phase shift, it is conveniently rejected by a polarizer. Finally, we must restrict ourselves to designs which represent practical solutions. For example, it is probably not practical to fabricate multi-layer achromatic retarders on the reflective addressing structure.

The design begins with the simplest rotative phase shifter (RPS) scheme, based on the quarter-wave half-wave quarter-wave (QHQ) variable retarder[6] shown in Figure 2b. Due to the symmetry of the structure, it is conveniently implemented in reflection as shown in Figure 2a. Assuming for the moment that both the quarter-wave and half-wave retarders are wavelength insensitive, the phase shift is twice the rotation angle of the half-wave retarder, (2α), and there is zero conversion to the orthogonal polarization. The complex transmittance for the ideal QHQ phase shifter can be obtained using Jones calculus. For an x polarized input/output this transmittance is given by

$$t_{xx} = e^{-i2\alpha} \quad . \tag{7}$$

For the CSLC material considered here, this represents a maximum phase shift of π radians, which is half the required modulation depth. In practice, the ideal phase only QHQ is not easily implemented. While it is practical to make the passive retarder(s) achromatic using a three layer Pancharatnam quarter-wave plate or possibly a Fresnel rhomb, the rotative element remains a CSLC device, which is chromatic. This structure is shown in Figure 2c. A benefit of this arrangement is that the field component that remains x-polarized is independent of wavelength. While the component that is converted to the y-polarization does not experience the desired phase shift, it is conveniently blocked with a polarizer. The retained field component has the complex transmittance

$$t_{xx} = \cos[\delta/2]e^{-i2\alpha} \quad . \tag{8}$$

Here δ is the deviation from the design retardation of π radians for the chromatic half-wave retarder. This term results in a decrease in amplitude for light at wavelengths other than the design wavelength of the half-wave retarder.

We also consider the case of a QHQ modulator which uses all zero-order waveplates. In this case, illustrated in Figure 2e, the x polarized component is contaminated by an additive term. Assuming that the quarter-wave and half-wave retarders have the same dispersion, the complex transmittance can be written as

$$t_{xx} = \cos[\delta/2]e^{-i2\alpha} + 2\sin^2[\delta/4]\left(2\cos^2[\delta/4] - \cos[2\alpha]\right) \quad . \tag{9}$$

In order to obtain a full 2π of phase shift, it is necessary to make two passes through a QHQ modulator, as shown in Figure 2g. Again assuming ideal achromatic waveplates, the output is a pure phase shift of 4α, or

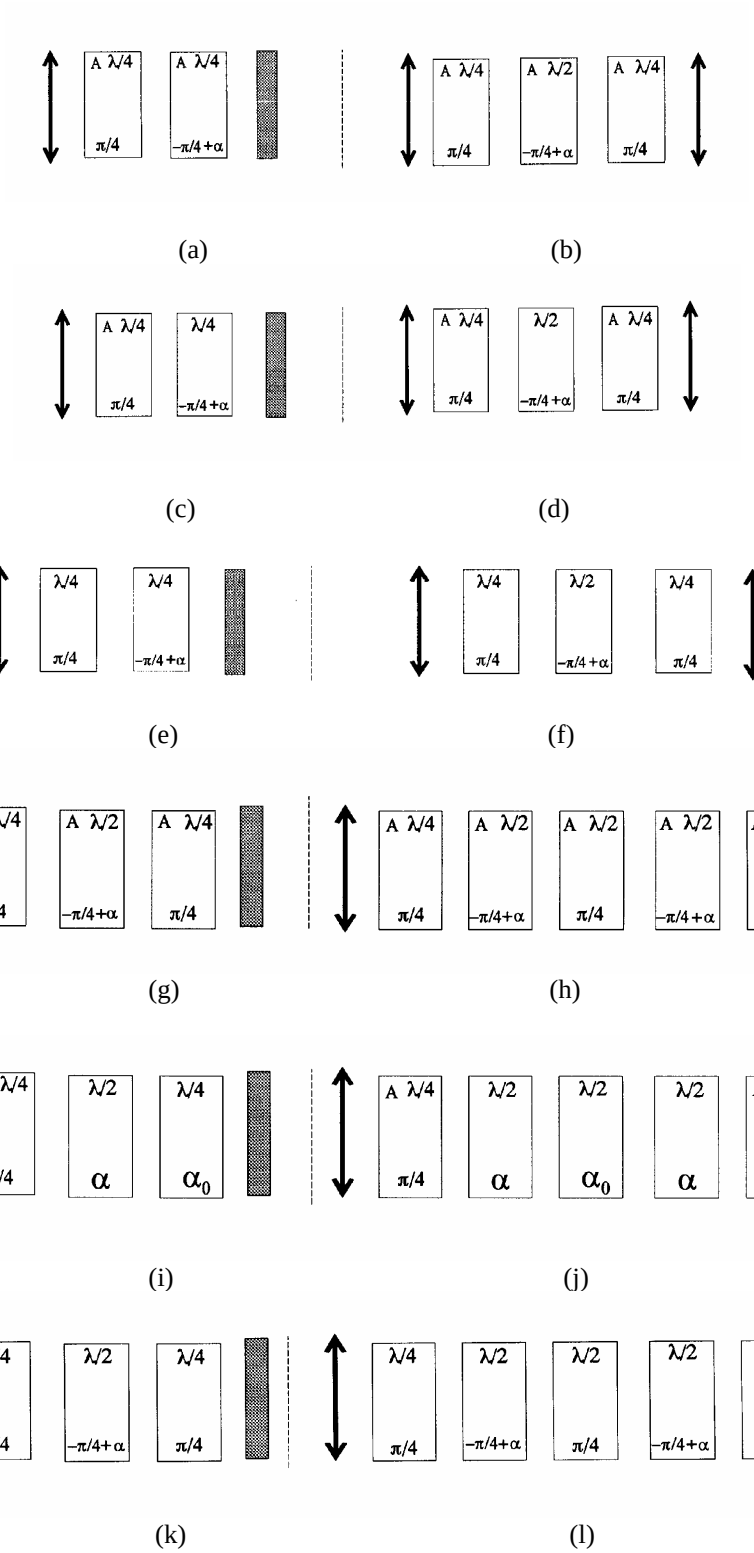

Figure 2. Reflection mode and unfolded phase shifter designs. (a) and (b) achromatic QHQ; (c) and (d) QHQ with a chromatic half-wave plate; (e) and (f) chromatic QHQ; (g) and (h) achromatic QHHQ; (i) and (j) QHHQ with chromatic half-wave plate, (k) and (l) QHHQ with all chromatic elements.

$$t_{xx} = e^{-i4\alpha} \quad . \tag{10}$$

It remains to select the specific rotation angles and the orientation of the passive polarization optics to achieve the optimum modulation in the event of a chromatic rotative device.

First consider the design of Figure 2i, which contains an achromatic quarter-wave retarder at the input. This is practical at the input, but is more problematic for the quarter-wave retarder on the mirror. Diffraction effects due to the path length between consecutive encounters with the pixelated half-wave retarder can significantly degrade performance. Also, the half-wave retarder must be electrically addressed across the quarter-wave retarder, increasing backplane voltage requirements and affecting electric field fringing. For these reasons, it is beneficial to minimize the thickness of the quarter-wave retarder. This probably rules out the use of a three layer Pancharatnam quarter-wave retarder on the mirror. While polymer cholesteric liquid crystal mirrors can be used[7], they are also fairly thick as high reflectors, and require high birefringence materials for broadband reflection. Such high birefringence cross-linkable liquid crystal polymers are not yet available.

Based on the above considerations, take the quarter-wave retarder on the mirror to be a zero-order waveplate with the same dispersion as the half-wave retarder. In this design, the range of tilt angles given by α, and the orientation of the passive quarter-wave retarder on the mirror given by α_0 can be selected to optimize performance. The optimum orientation is best illustrated using the unfolded version of Figure 2j.

The central three half-wave retarders of Figure 2j are the focus of the optimization. Recall that the achromatic compound half-wave retarder of Pancharatnam is formed using three zero-order half-wave retarders. The structure is achromatic when the two outside retarders are parallel to each other, at an angle of 60 ^{o} with respect to the central half-wave retarder. As the unfolded version shows, the two outside retarders are intrinsically parallel and rotate in unison. By properly selecting the passive retarder orientation, there are two states within the 90 ^{o} rotation of the outside retarders for which the three waveplates form a Pancharatnam achromatic half-wave retarder.

Consider the design with α_0 = 90 ^{o} and CSLC orientations of + 30 ^{o} and - 30 ^{o}. Both orientations satisfy the achromatic condition, the former giving a compound optic axis orientation of - 60 ^{o} and the latter an orientation of + 60 ^{o}. We thus have near ideal phase-only modulation in two orientations. Provided that we select this configuration, the CSLC molecules will rotate between + 45 ^{o} and - 45 ^{o} to achieve the desired modulation depth. We must therefore consider the behavior of the structure at orientations other than the two achromatic states given by $\alpha = \pm$ 30 ^{o}. At zero tilt, the outside retarders are crossed with respect to the passive retarder, yielding a net retardance of zero-order half-wave and an orientation of zero. This represents the worst-case amplitude loss for the modulator. Between the zero tilt state and the Pancharatnam orientation(s), there is an increase in the chromaticity of the phase induced by the structure. When the tilt angle exceeds the Pancharatnam condition, as required to obtain a full-wave of phase shift, there is also an increase in the phase chromaticity of the structure. However, the amplitude performance remains quite good out to $\pm$ 45 ^{o}, relative to the zero-tilt orientation.

Using Jones calculus, the complex transmission of the structure of Figure 2j can be written as

$$t_{xx} = \cos[\delta/2]\left(\cos^2[\delta/2]e^{i(2\alpha_0 - 4\alpha)} - \sin^2[\delta/2]\left[e^{-i2\alpha_0} + 2e^{-i2\alpha}\right]\right) \quad . \tag{11}$$

The output of the modulator for various tilt angles is given in Figures 3a and 3b. Our initial concern was that an increase in the number of chromatic retarders over the conventional QHQ modulator would take an additional toll on the chromaticity of the structure. Quite the contrary, we have found a structure in which the zero-order waveplates work together to significantly enhance the spectral response. At the worst-case tilt angle, the structure performs as well as the QHQ, with significantly better performance at other tilt angles. From an amplitude modulation standpoint, this structure performs better than the QHQ in general. However, as the error in retardation increases, the phase modulation depth decreases.

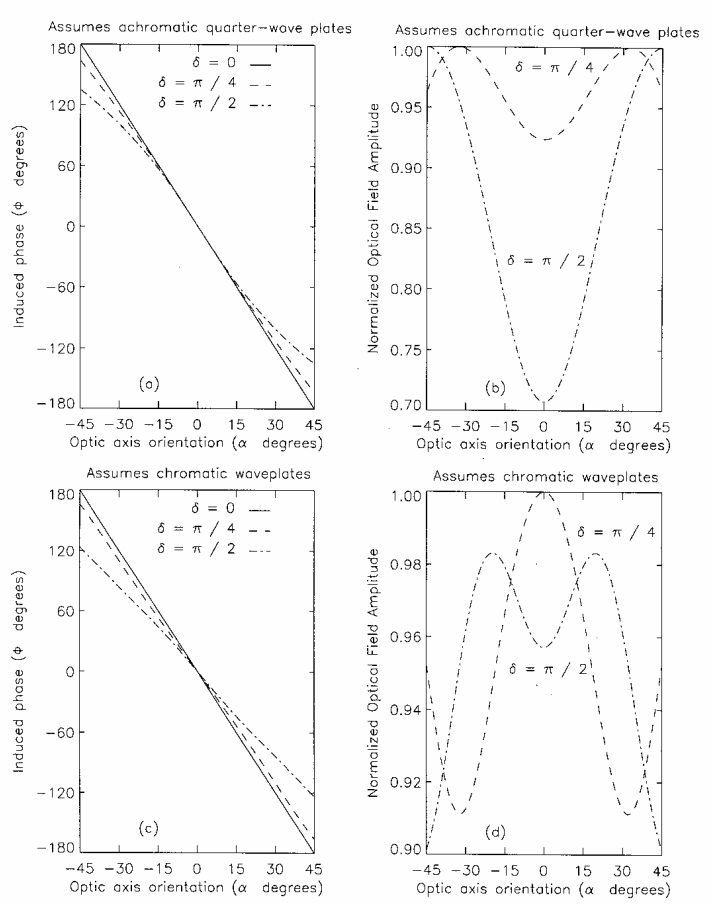

Figure 3. Complex transmittance of QHHQ. (a) and (b) phase and amplitude for the case of achromatic quarter-wave plates. (c) and (d) phase and amplitude assuming all chromatic elements.

For the results shown in Figure 3b, the amplitude modulation is less than 8% over the entire tilt range for a retardation error of $\delta = \pi/4$. Consider a central wavelength of 4 μm for the half-wave retarder, and assume no dispersion in the IR (not unreasonable away from absorption resonances) then a $\pi/4$ error in retardation corresponds to a wavelength range from 3 to 5 μm.

Note that, due to an odd number of zero-order half-wave plates, the structure of Figure 2j can never achieve a zero-retardance state. In order to achieve this, the input (and exit) quarter-wave retarder(s) must also be zero order. Consider the unfolded design of Figure 2*l*, where the central half-wave retarder is parallel to the outside quarter-wave retarders. When the active structure is crossed with these three waveplates, the net retardance is identically zero at all wavelengths. Note that the structure is much like that of Figure 2j in that the half-wave plates modulate about the crossed retarder configuration.

The transmission of the QHHQ assuming all chromatic elements is given by

$$
\begin{aligned}
t_{xx} = {} & \frac{1}{2}\sin^2[\delta/2]\left(1+3\cos[\delta]\right) - \cos[\delta/4]\sin[3\delta/4]\sin[\delta]e^{-i2\alpha} \\
& - \sin[\delta/4]\cos[3\delta/4]\cos[\delta/2]e^{i2\alpha} + \sin^2[\delta/4]\cos^3[\delta/2]\, e^{i4\alpha} \\
& - \cos^2[\delta/4]\cos^3[\delta/2]e^{-i4\alpha}.
\end{aligned}
\tag{12}
$$

Transmission and phase curves are given in Figures 3c and 3d for this structure. The amplitude modulation is 10% or less for the entire tilt angle range for retardation errors as large as 50%. However, for a retardation error of 50% the phase modulation depth has decreased to 240 ^{o}. While the all chromatic structure of Figure 2*l* offers a true zero retardation state and excellent amplitude modulation characteristics for large retardation error, the structure of Figure 2j performs better for a retardation error of $\delta = \pi/4$ or less.

2.3 Polymer nematic liquid crystal retarders

To obtain a passive quarter-wave retarder having dispersion characteristics similar to the active half-wave retarder material we have turned to polymer nematic liquid crystals (PNLC). These crosslinkable liquid crystal silicones can be fabricated into zero-order retarders on a single substrate. Figure 4 shows the transmission for a quarter-wave Fresnel rhomb in series with a homogeneous aligned PNLC retarder deposited onto a single substrate The retarder and rhomb were oriented at 0 ^{o} between parallel polarizers at 45 ^{o}. The null in the transmission spectra indicates that this particular PNLC film acts as a zero-order quarter-wave retarder at 1250 nm. This near-IR PNLC retarder is approximately 2.5 μm thick.

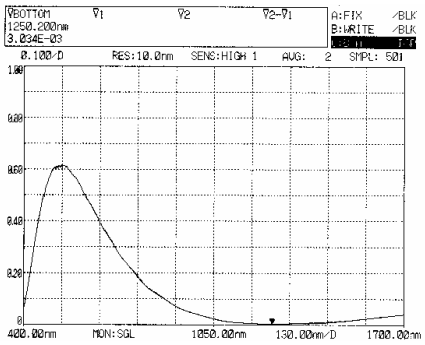

Figure 4. Transmission of PNLC film and Fresnel rhomb between parallel polarizers.

2.4 Spatial light modulator experiments

In this section we demonstrate a liquid crystal grating which modulates phase achromatically at visible wavelengths. This is accomplished using a CSLC SLM of 256x256 pixels which is a zero order quarter-wave retarder at 570 nm. On reflection, this device acts as a rotative half-wave plate. The pixel pitch is 21 μm. The SLM modulates the light using polarization manipulation. For the case considered here linearly polarized light is incident on the SLM. Depending on the pattern written to the SLM, it acts as a binary amplitude or phase grating. For the amplitude grating, the CSLC optic axis is either parallel to the incident polarization (producing a bright state) or at 45 ^{o} (resulting in a 90 ^{o} rotation of the polarization and a dark state). For the binary phase grating the optic axis of the CSLC alternates between orientations of 22.5 ^{o} and 67.5 ^{o} with respect to the incident polarization yielding 0 and π radians of phase, respectively.

Figure 5 is a series of photographs showing the white light operation of the SLM. The first column shows the information written to the SLM. This is either an amplitude or phase grating and has a period of 672 μm or 42 μm. Each row shows the far field diffraction patterns due to the corresponding SLM addressing shown in the first column. The second column shows binary amplitude modulation, the third column shows binary phase modulation. Note that in the third column the zero order diffraction is absent for the diffraction patterns due to the phase grating. The wavelength spread due to propagation to the far field is more evident for high spatial frequencies as demonstrated in columns 2 and 3 of the third row.

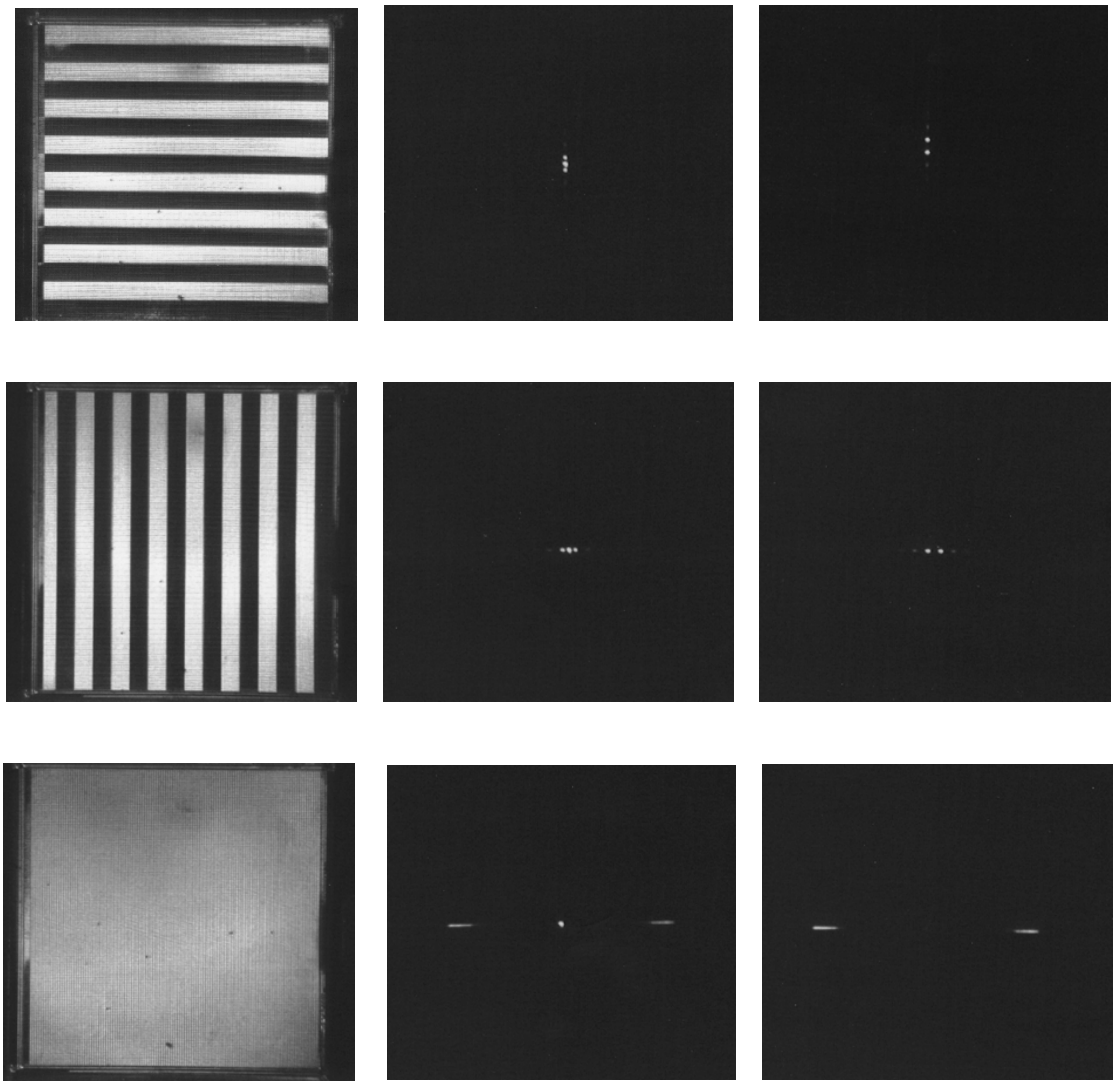

Figure 5. First column shows the SLM addressing; second column: far field diffraction pattern for a binary amplitude grating; third column: far field diffraction pattern for a binary phase grating.

Figure 6 compares the operation of the phase masks for monochromatic light and band limited white light. Each row corresponds to a given phase pattern written to the SLM, while each column corresponds to a different wavelength range. The image of the phase mask used to obtain the data in each row corresponds to the pattern written to the SLM shown in the same row of the first column of Figure 5. The white light patterns in columns 2 and 3 can be compared to the monochromatic pattern in the corresponding row of column 1. First, for low spatial frequencies, the grating dispersion is not very noticeable. This is demonstrated by the relatively uniform first order spots of the diffraction patterns shown in the first and second rows of columns 2 and 3. The wavelength dispersion gets much worse for high spatial frequencies as shown in the third row. Without compensation, white light can only be steered to small angles. Finally, note that the efficiency of the phase grating is band limited. The patterns in the third column (which are due to incident light having a 700 nm bandwidth from the visible to near IR) show some light leaking into the zero order of the far field pattern. This is a manifestation of the chromaticity of the CSLC retarder.

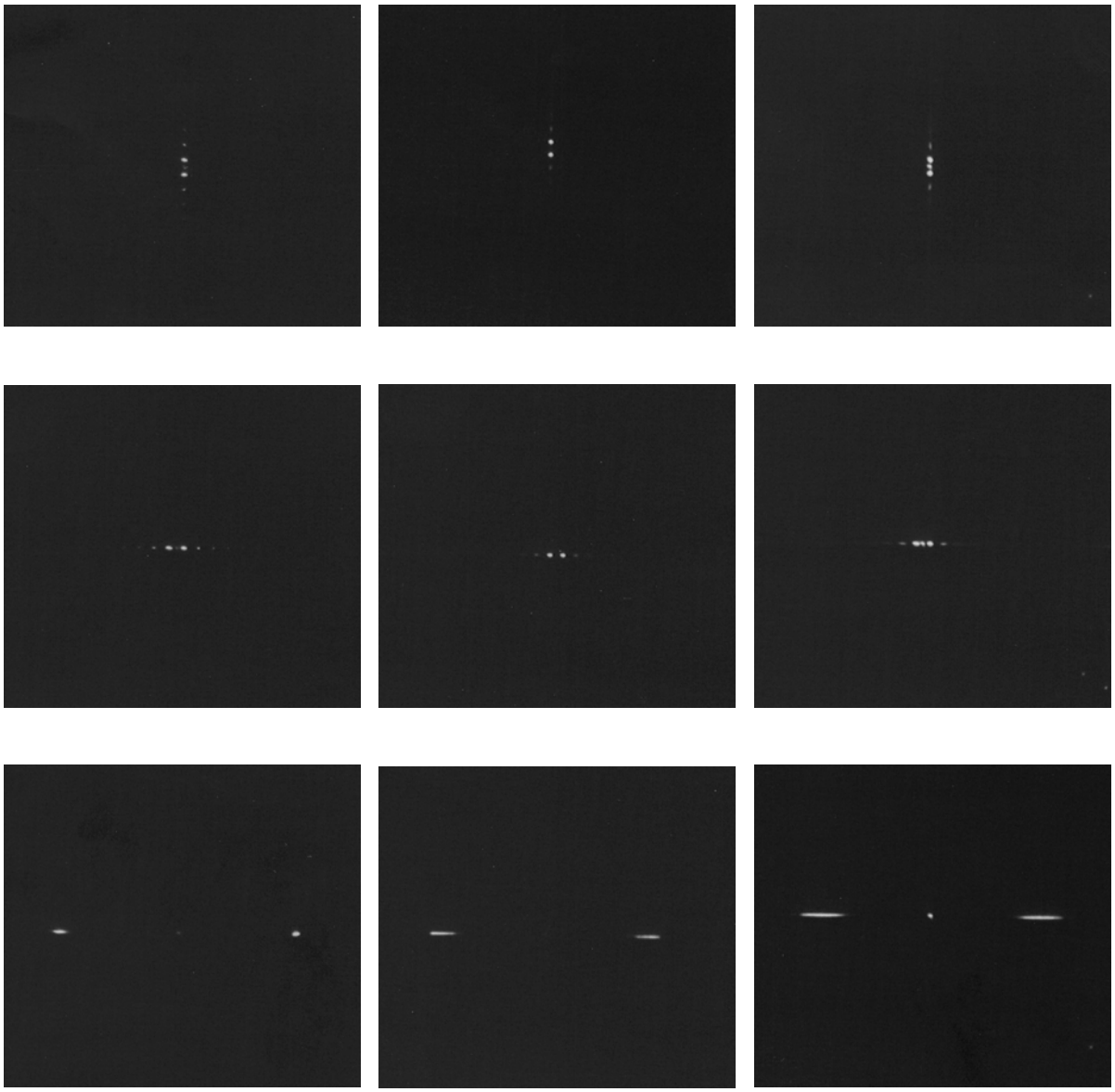

Figure 6. Diffraction patterns for binary phase written to the SLM, first column, monochromatic light (685 nm); second column, white light (400 nm to 650 nm); third column, white light, (400 nm to 1100 nm). Each row corresponds to the pattern in the same row of the first column in the previous figure (Figure 5).

3. ACHROMATIC FOURIER TRANSFORM SYSTEM

The basic design criterion for a Fourier transform lens is that the image height in the Fourier transform (or image) plane is equal to the product of the focal length and the sine of the input angle. There may also be an added requirement that there exist no phase curvature in the Fourier transform plane. The former requirement ensures that the spatial frequency components in the object are linearly mapped to positions in the Fourier plane and is a direct result of the grating equation. The latter requirement ensures that the Fourier transform operation is not limited to intensity but includes phase information as well. Both of these design criteria have been met for the current broadband system which has been designed to operate within the visible spectrum.

3.1 Design description

The basic layout which is similar to that discussed by Morris[4], consists of three lens groups and is shown below in Figure 7. Given the dispersive nature of the input grating, the power of the lens system has been designed to be proportional to the wavelength. This ensures that the image height in the Fourier plane is fixed for all wavelengths. The first group consists of a refractive doublet and a single diffractive surface located on a planar surface. This lens group is highly chromatic with a lens power that decreases with wavelength. This chromatic behavior allows for the red marginal ray height at the second lens group to be larger than the corresponding blue marginal ray height. This is necessary to fulfill for the simultaneous requirements that the power of the entire Fourier transform lens increases with wavelength and that the longitudinal chromatic aberration is corrected[8].

Figure 7. Achromatic Fourier transformer.

The second lens group consists of five refractive elements and includes a single diffractive surface located on a planar surface. It is important to note that this group is nearly symmetric and in fact the entire Fourier lens is approximately symmetric about the central diffractive surface (the third lens group is identical to the first lens group). This symmetry in effect eliminates the phase curvature which might otherwise be present in the transform plane. Incidentally, this symmetry also eases the fabrication requirements since there are only five distinct refractive designs and two distinct diffractive designs.

3.2 Basic design specifications

Design Spectral Band = 535 nm to 650 nm;

Focal length = 212.53 mm (at 593 nm);

Stop Diameter (located at the first lens surface) = 14 mm;

F-number = 14.3;

Minimum input grating period = 28 μm (height in transform plane = 4.34 mm);

System Length = 675 mm.

3.3 Performance results

The ray fan shown in Figure 8 depicts performance for an input grating period of 28 μm which corresponds to the worst performance. The image height in the transform plane for this grating period is 4.34 mm. Given that the Airy disc spot diameter for λ = 535 nm is equal to 19 μm, one can see that the system is essentially diffraction limited.

The lateral color will be defined as the difference in image heights for the central wavelength (λ = 593 nm) and some other wavelength. The image height for a given wavelength is taken as the height of the geometrical centroid. The maximum error shown in Figure 9 corresponds to approximately 16% of the Airy disc diameter. The image height, Y, as a function of input angle, θ, must be related to the focal length, f, as $Y = f \sin \theta$. For a focal length, f = 212.53 mm, the deviation from this relationship is determined to be $\pm$ 1 μm at the design wavelength of 593 nm for grating periods down to 28 μm. Again, the image height is taken as the height of the geometrical centroid.

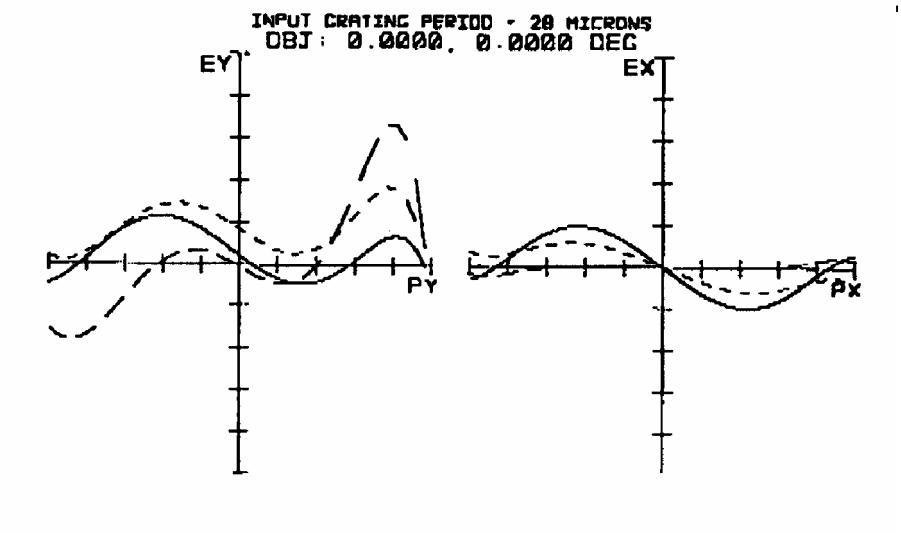

Figure 8. Image height in the transform plane for a 28 μm grating period.

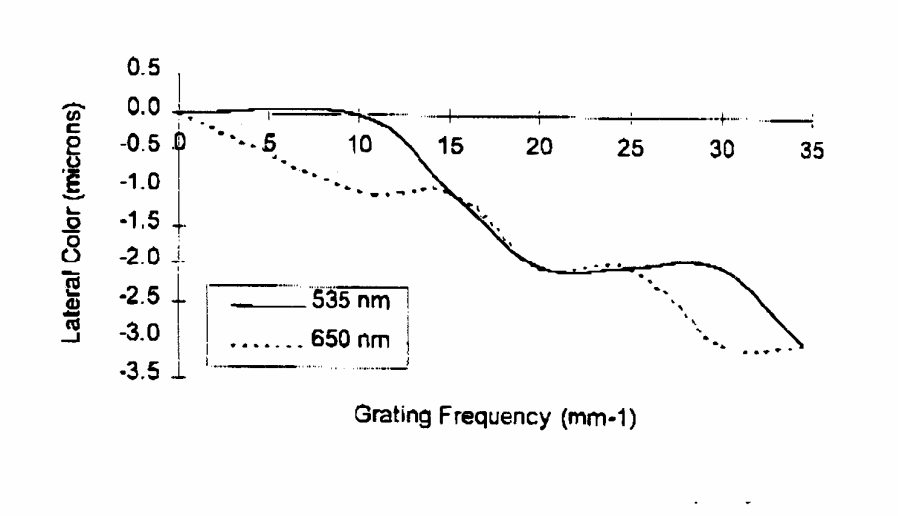

Figure 9. Lateral color as a function of grating frequency.

4. EXTENSION TO MID-INFRARED WAVELENGTHS

In order to scan thermal images, the wavelength range of operation should cover the 3 to 5 μm spectral region. This will require a half-wave retarder of CSLC on the order of 20 μm thick. Because the IR retarder thickness is slightly larger than the material pitch, a 20 μm thick CSLC cell obtained using conventional alignment techniques exhibits poor contrast and scatters incident light. However, alignment is possible using special techniques, such as photo-alignment and electric field treatment. A 22 μm thick cell which uses a hybrid alignment technique has produced the best results to date. A 4 mm x 12

mm area exhibited uniform alignment and essentially no scatter. Another important issue is absorption of the CSLC and PNLC materials in the 3-5 μm band. A CSLC cell of approximately 20 μm thickness was fabricated between CaF_2 substrates and measured using a Fourier-transform infrared spectrometer. The peak absorption is at 3.4 μm with a smaller resonance at 3.5 μm. This is likely due to a C-H bond which is common to most liquid crystal materials. Relatively high transmittances starting from 60% at a wavelength of 3.6 μm and steadily increasing to 80% at 5.7 μm characterize the remainder of the measured spectrum. For the PNLC material the maximum absorption also occurs at 3.4 μm but decreases rapidly and remains low throughout the remainder of the spectral band. These results indicate that a mid-IR modulator is possible using existing liquid crystal materials.

5. SUMMARY AND CONCLUSIONS

A broadband beam scanning system has been discussed. The design of the beam steerer calls for an array of achromatic modulators and an achromatic Fourier transform lens system. The modulating elements consist of a half-wave CSLC retarder and a passive PNLC quarter-wave plate on a mirror. Because these devices use polarization modulation to achieve a phase shift, they operate over a broad spectral band. Modulator designs which produce an achromatic phase shift have been analyzed using Jones calculus. A reflection mode device consisting of an achromatic input quarter-wave plate, a CSLC half-wave retarder, and a passive quarter-wave retarder having the same dispersion characteristics as the half-wave retarder exhibits the best performance for the application considered here. An SLM which uses polarization modulation to diffract incident light has demonstrated broadband characteristics. A Fourier transform lens design for the visible spectrum has been detailed and the feasibility of the modulator technology at mid-IR wavelengths was addressed.

6. ACKNOWLEDGMENTS

This work is supported by Wright Laboratory, Wright-Patterson United States Air Force Base through the small business technology transfer (STTR) program. Contract number F33615-96-C-1965

7. REFERENCES

1. D. P. Resler, D. S. Hobbs, R. C. Sharp, L. J. Friedman, and T. A. Dorschner, "High-efficiency liquid-crystal optical phased-array beam steering," Opt. Lett., Vol. 21, 689-691, (1996).

2. P. F. McManamon, E. A. Watson, T. A. Dorschner, and L. J. Barnes, "Applications look at the use of liquid crystal writable gratings for steering passive radiation," Opt. Eng., Vol. 32, 2657-2664, (1993).

3. E. A. Watson, P. F. McManamon, L. J. Barnes, and A. J. Carney, "Applications of dynamic gratings to broad spectral band beam steering," SPIE Vol. 2120 Laser Beam Propagation and Control (1994).

4. G. M. Morris, "Diffraction Theory for an achromatic Fourier transformation," Appl. Opt. Vol. 20, (1981)

5. G. M. Morris, and D. A. Zweig, "White Light Fourier Transforms," in Optical Signal Processing, J.J. Horner, ed. (Academic Press New York, 1987) Chapter 1.2.

6. G. D. Sharp, "Chiral smectic liquid crystal tunable optical filters and modulators," Ph. D. Thesis, University of Colorado 1992.

7. J. E. Stockley, G. D. Sharp, S. A. Serati, and K. M. Johnson, "Analog optical phase modulator based on chiral smectic and polymer cholesteric liquid crystals," Opt. Lett. Vol. 20 2441-2443, (1995).

8. R. E. Hopkins and G. M. Morris, "White light Fourier transform lens," Kinam., Ser. C, Vol. 5, 135-149 (1983).